Laser irradiation for controlling size of TiO_2–Zeolite nanocomposite in removal of 2,4-dichlorophenoxyacetic acid herbicide

Fatemeh Abdollah, Seyed Mehdi Borghei, Elham Moniri, Salimeh Kimiagar and Homayon Ahmad Panahi

ABSTRACT

This study focused on the synthesis of TiO_2–Zeolite nanocomposite through a sol–gel approach. The decrease in the size of the nanocomposite is considered a primary parameter to improve photocatalytic activity. In this regard, fabricated samples were exposed to laser irradiation (532 nm) for four different time intervals in order to investigate the size variation of the nanocomposite. FTIR, UV–Vis, XRD, DLS, SEM and EDX analyses were applied to characterize and determine the size of the products. An optimized nanocomposite sample, in term of the particle size, was used for photodegradation of 2,4-D herbicide from aqueous solution. Photodegradation was carried out under UV irradiation (12 W) and Xe lamp irradiation (200 W). The obtained results showed that laser irradiation time has a substantial effect on controlling the size of the nanocomposite. Results from the photocatalyst study indicated that the elimination of 2,4-D under the Xe lamp irradiation was higher compared with the UV irradiation. Also, the final synthesized nanocomposite exhibited higher catalytic activity for photodegradation of 2,4-D compared with pure Zeolite and pure anatase TiO_2 samples. The reusability of TiO_2–Zeolite nanocomposite was studied in four successive cycles to evaluate the removal of 2,4-D under UV irradiation.

Key words | 2,4-D, laser irradiation, nanocomposite, photocatalyst, TiO_2, zeolite

Fatemeh Abdollah
Department of Environmental Engineering, Faculty of Natural Resources and Environment, Science and Research Branch,
Islamic Azad University,
Tehran,
Iran

Seyed Mehdi Borghei
Department of Chemical and Petroleum Engineering,
Sharif University of Technology,
Tehran,
Iran

Elham Moniri (corresponding author)
Department of Chemistry, Varamin (Pishva) Branch,
Islamic Azad University,
Pishva,
Iran
E-mail: *moniri30003000@yahoo.com*

Salimeh Kimiagar
Nano Research Laboratory (NRL), Physics Department, Central Tehran Branch,
Islamic Azad University,
Tehran,
Iran

Homayon Ahmad Panahi
Department of Chemistry, Central Tehran Branch,
Islamic Azad University,
Tehran,
Iran

INTRODUCTION

In the last decade, a diverse range of drugs, pesticides such as herbicides, hormones and some chemical products have appeared in wastewater and water resources. These compounds are called emerging pollutants (Tobajas *et al.* 2017). The emerging pollutants are a significant group of organic pollutants for the scientific community. They have to be controlled and minimized on the surface and in ground water resources (Nejati *et al.* 2013). They could be potentially hazardous, due to being endocrine disruptors and their release process cannot be controlled easily. This phenomenon happens because high quantities of these pollutants are used worldwide (Tobajas *et al.* 2017). Recently, these pollutants were defined as compounds that needed advance instrumental analysis to be detected precisely. Controlling and monitoring strategies have not been proficient up until now (la Farré *et al.* 2008). Among emerging pollutants such as herbicides, 2,4-dichlorophenoxyacetic acid (2,4-D) is immensely applied among herbicides in order to control broad leaf plants in agriculture, forestry, and aquatic vegetation. In the commercial market over 600 types of 2,4-D are produced with the purpose of controlling weeds. Since 1968, 2,4-D has been widely used in Iran. Approximately 530 tons of the herbicides are used annually in Iran, and 20%–30% of them belong to 2,4-D (Agricultural Ministry

doi: 10.2166/wst.2019.333

2012). In addition, 2,4-D residuals have been reported at around 3 mg L^{-1} in raw agricultural drainage water of south Iran (Jaafarzadeh *et al.* 2018). However, it has been extensively used in agriculture, because of its low cost, excellent performance, and high solubility in water. A high consumption rate leads to considerable harm to public health and the environment (Lemus *et al.* 2008). It has recently become a serious environmental concern; 2,4-D is classified as a probable carcinogen and mutagen compound by the International Agency for Research on Cancer (IARC). The maximum permitted 2,4-D concentration in drinking water is a recommended 70 μg L^{-1} by the World Health Organization (WHO) (Ding *et al.* 2012). Therefore, the degradation of 2,4-D has been a significant worldwide challenge. Hence, the expansion of cheap and environmentally friendly methods is necessary for reducing 2,4-D in the aquatic environment. Lately, photocatalytic development has shown great potential to degrade organic contamination and deliver the total decrement of toxic constituents (Deveau *et al.* 2007).

The application of nanoparticles for cleaning up contaminants in air, soil, and water can be considered as one of the most promising environmental technologies. TiO_2 is known as one of the best semiconductors used as a photocatalyst for pollutant degradation in the liquid phase. TiO_2 has been used for purification and water treatment due to its excellent and extensive advantages of high efficiency, nontoxicity, chemical stability, suitable band energy level and low price. TiO_2 nanoparticles are typically used due to their high specific surface area and higher surface reaction rate to degrade pollutants (Chong *et al.* 2009). Therefore, TiO_2 nanoparticles could efficiently participate in the photodegradation of organic pollutants through the treatment process. Semiconductor materials can absorb UV light due to a large band gap. Therefore, many efforts have been made to design highly efficient photocatalysts, which can work under visible-light irradiation. Titania particles exhibit a blue shift in their absorption spectrum due to quantum size effects which cause different excitation energies. This phenomenon is also observed for molecular TiO_2 species. The blue shift refers to the band gap broadening of the semiconductor (Anpo *et al.* 1987). Therefore, various publications dealing with TiO_2–Zeolite nanocomposite have linked the observed blue shift to the quantum-sized Titanium particles (Liu *et al.* 1993). Recently, researchers have preferred to support TiO_2 nanoparticles using a porous natural mineral such as Zeolite, and other porous materials. Among various materials supporting TiO_2, Zeolites have been proposed because of uniform and unique pores, super adsorption capability and the particular ion-exchange ability of the Zeolite (Taheri Najafabadi & Taghipore 2014). The combination of TiO_2 and Zeolite is achieved by applying different approaches, such as wet impregnation and sol-gel processes. In this study, we synthesized TiO_2–Zeolite nanocomposite by using the sol–gel method and studied the size control condition to improve the photocatalytic activity of the nanoparticles for the removal of 2,4-D.

MATERIALS AND METHODS

Materials

The natural Zeolite clinoptilolite was obtained from Semnan province of Iran. TiO_2 and 2,4-D ($C_8H_6Cl_2O_3$) with a purity of >98% were purchased from Merck company.

Synthesis of TiO_2–Zeolite nanocomposite

TiO_2–Zeolite nanocomposite was synthesized using the sol–gel method. Briefly, 0.1 g TiO_2 and 0.1 g Zeolite were dispersed in 15 mL of distilled water under vigorous stirring (30 min). The mixture was stirred continuously at 40 °C for 4 h until the mixture became a milky white color, which eventually turned to a transparent homogeneous sol with no visible precipitation. Five separate sols in different beakers were prepared, then each beaker was separately exposed to irradiation under an Nd:YAG pulsed laser system (Quantel, Brilliant b class 4 with 532 nm wavelength, 5 ns pulse duration, 10 Hz repetition rate, 90 mJ maximum pulse energy and 7 mm beam diameter) at its second harmonic to fabricate nanocomposite with different sizes. Various irradiation times, 0, 3, 5, 7 and 10 min, were applied for five beakers, separately.

Photocatalytic experiments

Photocatalysis experiments were carried out with the beaker being shaken at 600 rpm using a laboratory-designed photodegradation reactor (Figure 1). All experiments were performed at room temperature. The beaker was isolated from the environment in order not to receive extra light from other sources and to collect light from one direct source. The distance between the lamp and photocatalysis system was about 5 cm. All the experiments were carried out in a dark room to eliminate extra lights. The initial

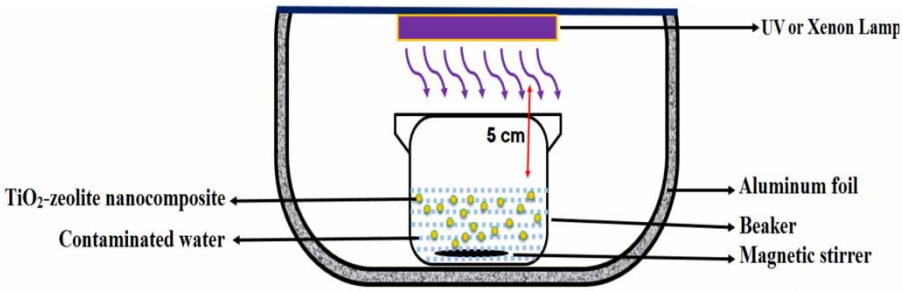

Figure 1 | Schematic of laboratory-designed photodegradation reactor.

concentration of the 2,4-D solution was 10 mg L^{-1} in deionized water.

The TiO_2–Zeolite nanocomposite was added to 500 ml of solution with a concentration of 0.4 g L^{-1}. The solutions were kept in the dark while being stirred for 30 min, in order to achieve adsorption–desorption equilibrium between the 2,4-D and photocatalyst nanocomposite. Then, the beaker was exposed to the UV irradiation (12 W) and Xe lamp irradiation (200 W). After 5, 10, 20, 40 and 80 minutes' time interval, 5 mL of the solution was taken, and filtered through a 0.22 μm syringe filter to remove the catalyst powder. The concentration profile changes were determined by the absorbance at 283 nm. Ten solutions of 2,4-D with concentrations between 0.1 and 60 mg L^{-1} were prepared to find the 2,4-D maximum absorption (283 nm). The same process was repeated for pure Zeolite and pure anatase TiO_2 samples. The following equation was used to calculate the removal efficiency of the 2,4-D:

$$Removal\% = [1 - C_t/C_0] \times 100 \quad (1)$$

where C_0 and C_t are the concentrations of 2,4-D in the solution before ($t = 0$) and after exposure time t under irradiation, respectively.

Reusability

The reusability of the TiO_2–Zeolite nanocomposite was studied by repetitive experiments as follows. For each run, a solution of 2,4-D (10 mg L^{-1}) was prepared and then mixed with 0.05 g of TiO_2–Zeolite nanocomposite while being stirred (600 rpm) for 5 min in a dark room at room temperature. Then the sol was placed under the UV irradiation (12 W) using a laboratory-designed photodegradation reactor for 20 min. After the reaction time (20 min), 5 mL of the solution was taken and centrifuged. Then the removal of 2,4-D was determined by the UV–Vis spectrophotometer and using Equation (1) (R_1 run). After each experiment, the TiO_2–Zeolite nanocomposite was separated by centrifuge and then washed by 10 mL pure methanol and 10 mL deionized water. The centrifuging and washing process was repeated two times. The samples were subsequently further used for the experiment with the same previous conditions. These processes were repeated four times (R_1, R_2, R_3, up to R_4 run).

Characterization

The samples were characterized by Fourier transform infrared spectroscopy (FTIR, Nicolet 6700 spectrometer), UV–Vis absorption spectra (Perkin Elmer spectrometer) and X-ray diffraction (XRD, Cu, Ka1 = 1.5405, STOE STADI, MP, GERMANY). The size of nanocomposite was determined by dynamic light scattering (DLS, Malvern Instruments MAL1008078). Scanning electron microscopy (SEM) and energy-dispersive X-ray spectroscopy (EDX, VEGA/TESCAN-XMU) illustrated the morphology of the nanocomposite.

RESULT AND DISCUSSIONS

Fourier transform infrared spectroscopy (FTIR) was used for identification of the chemical bonds in the TiO_2–Zeolite nanocomposite (Figure 2(a)–2(f)).

The peaks at 3,434 cm^{-1} and 1,642 cm^{-1} are due to the stretching vibration of the hydroxyl groups (O-H bonds) and the bending vibration of the free water molecules in the Zeolite chemical structure, respectively. The peaks at 550 cm^{-1} and 700 cm^{-1} are known to be stretching vibrations of Ti-O-Ti bonds (Haque *et al.* 2017). Also, the sharp peak around 1,070 cm^{-1} is attributed to the asymmetric stretching vibrations of Si-O-Si which could be covered by the Al-O-Si and Al-O stretching in the Zeolite. Based on the previous reports, by importing metal cations into the Zeolite framework, the position of absorption bands could be shifted slightly, such as the Si-O-Si vibration around 1,000 cm^{-1} (Trujillo *et al.* 2013). The presence of

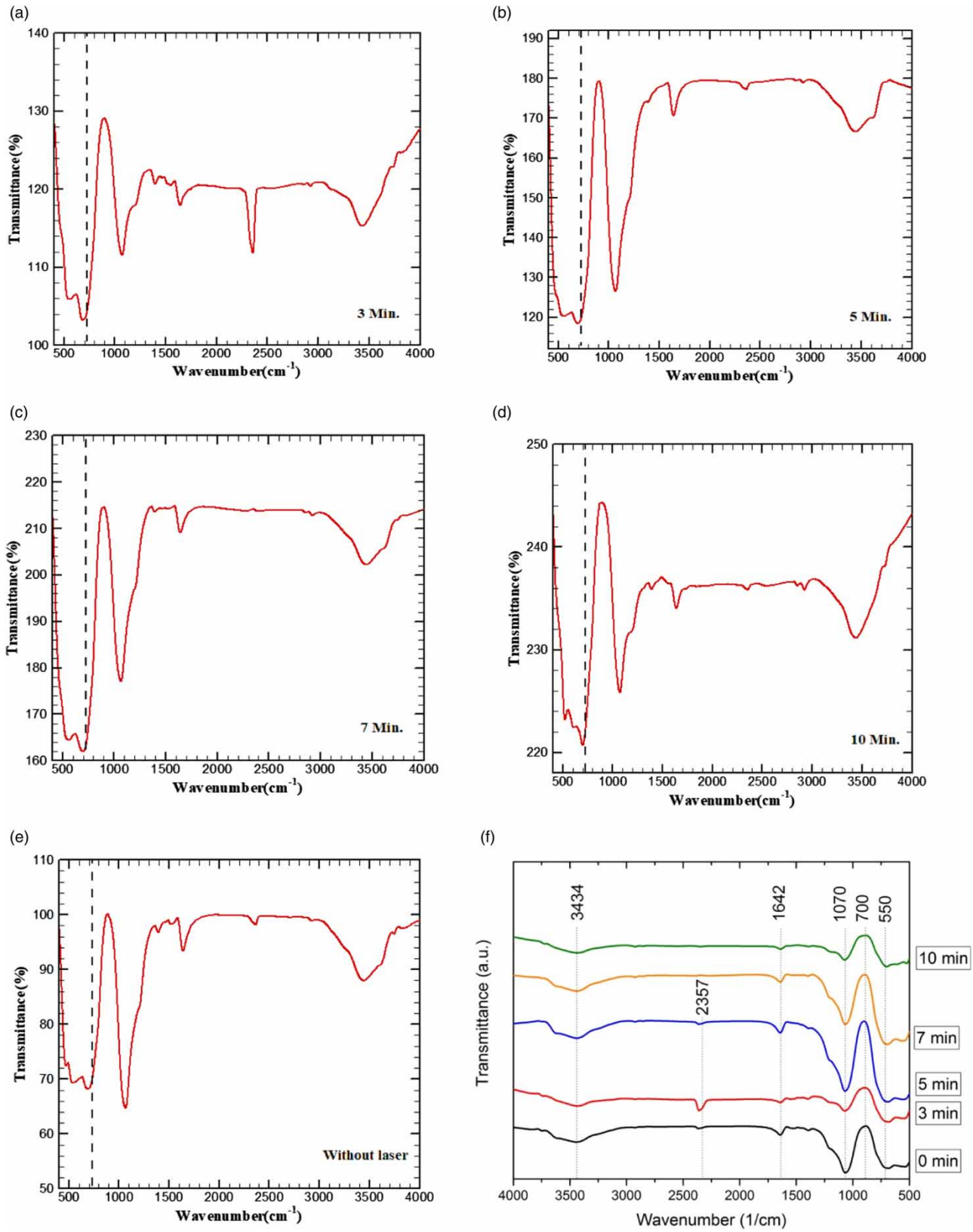

Figure 2 | FTIR spectra of the sample with: (a) 3, (b) 5, (c) 7, (d) 10, and (e) 0 min laser irradiation; (f) comparison of all the nanocomposites.

metal cations could explain this variation in Zeolite structure after the synthesis of the nanocomposite (Yener *et al.* 2017). No peak is observed in the range near 960 cm^{-1} which is related to the asymmetric stretching vibration of Ti-O-Si. The absence of this peak indicates that the TiO_2 has been sited on the surface of the Zeolite framework (Hassan Alwash *et al.* 2013). Therefore, TiO_2 is limited to SiO_4 or AlO_4 in the Zeolite structure, and it might cause overlapping of these peaks in FTIR (Yener *et al.* 2017).

Figure 3 shows the XRD pattern of the TiO_2–Zeolite before and after laser irradiation (532 nm). As is seen, all the obtained peaks are assigned to the anatase crystalline phase of TiO_2 (JCPDS No. 01-071-1166). The main diffraction peaks are (101), (112), (200), (105), (211), (204), (116), (220), (301), and (312). The obtained XRD pattern of the nanocomposite denotes that the diffraction peaks found to be (020), (111), (400), (422) and (151) correspond to the data listed for clinoptilolite (JCPDS No. 00-025-1349).

No constituent of impurities was detected based on the XRD pattern. The above results revealed that by increasing laser time, the obtained peaks such as (020), (111), (400), (101), (105), (200) and (211) in the nanocomposite become sharper and broader. Also, the intensity of the peaks after laser irradiation is stronger compared with the nanocomposite with no irradiation. Furthermore, no diffraction peaks corresponding to the typical TiO_2 phase are found. This phenomenon may suggest that the loading content of TiO_2 into the Zeolite is too minor to be detected by XRD analysis (Liu *et al.* 2014). In the synthesis procedure, TiO_2 almost covered the surface of the clinoptilolite and inhibited the peaks of the clinoptilolite from being detected by XRD (Yener *et al.* 2017). Mainly, the peaks correspond to the (101), (200) and (211) planes. Based on these results it can be inferred that the Zeolite was successfully doped by TiO_2.

The average crystal size (D) for the nanocomposite was calculated based on Debye Scherrer's equation, $D = \frac{K\lambda}{FWHM \times \cos\theta}$, where $K = 0.89$, λ is the X-ray wavelength (1.54 Å), FWHM is the full width at half-maximum of the diffraction line in radians and θ is the diffraction angle of the XRD spectra. The average crystal size of the nanocomposite decreased from 30 nm to 28 nm for $t = 0$ and $t = 7$ min laser irradiation time, respectively. It is consistent with the results of the SEM micrographs.

Figure 4 displays UV–Vis absorption spectra of the TiO_2–Zeolite at different laser irradiation times. The TiO_2–Zeolite samples exhibit UV light absorbance below 800 nm, which is assigned to the electronic transition from the O_{2p} orbital to the Ti_{3d} orbital (Cheng *et al.* 2014). However, by increasing laser irradiation time, light absorbance in the visible-light region is significantly enhanced. Also, a shoulder at 310 nm, which can be assigned to UV absorbance, disappeared after laser irradiation, which means the sample gained more visible-light absorbance properties.

The dynamic light scattering (DLS) technique was applied to determine the size of the nanocomposite at time = 0, 3, 5, 7 and 10 min laser irradiation (532 nm). The results are presented in Table 1.

It is clear that by increasing the irradiation time, the size of the nanocomposite decreased; however, at $t = 10$ min, the size of the nanocomposite increased (Table 1). The smallest

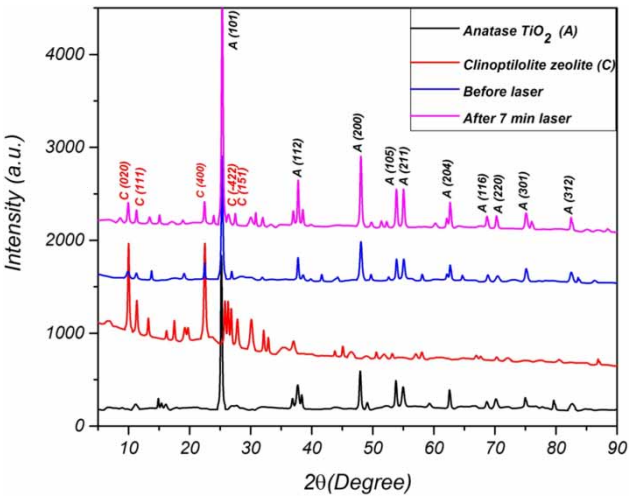

Figure 3 | XRD spectrum of the synthesized nanocomposite at $t = 0$ and $t = 7$ min laser irradiation (532 nm).

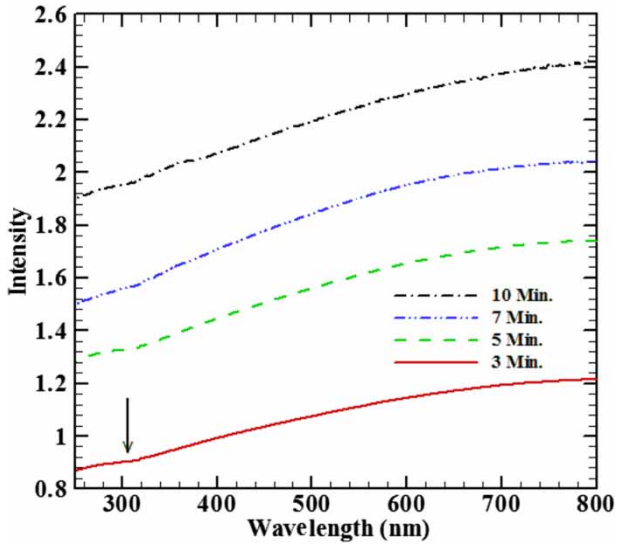

Figure 4 | UV–Vis absorption spectra of the nanocomposite at different laser irradiation times.

Table 1 | Size of the nanocomposite

Time (min)	Particle size (nm)
0 (laser off)	222
3	210
5	185
7	157
10	299

particle size observed is for 7 min laser irradiation, which is about 157 nm. The effect of the intensity and pulse length of the laser radiation on the nanoparticle appears in three mechanisms: heating, melting or evaporating the sample. The particles coalesce with each other during the photothermal melting step and form more significant aggregated structures. In the case of heating, annealing occurs for the sample. There are two ways of changing the particle size: (1) thermal annealing at temperatures between 550 and 650 °C leads to an increase of the particle size; (2) pulsed laser irradiation at 266 nm wavelength acts oppositely, yielding smaller-sized particles (Sendova *et al.* 2006). In order to control the particle size it is possible to use these two ways until one achieves the suitable particle size (Sendova *et al.* 2006). Another possible mechanism is fragmentation and ionization of the nanoparticle, leading to a surface charge which in turn causes it to be disjointed into smaller particles (Kamat *et al.* 1998). The process that is called separation or dissociation of a nanoparticle has been detected for free particles or particles on a surface (Kamat *et al.* 1998). However, the morphology of nanoparticles is altered by laser irradiation, and the detailed mechanisms of laser–colloidal particle transformation are not defined at present. Also, the interaction mechanism of the nanoparticles with laser radiation is not yet fully understood. Therefore, further investigation with improved techniques is necessary.

Figure 5(a)–5(e) shows the SEM images of synthesized nanocomposite at 0, 3, 5, 7 and 10 min laser irradiation

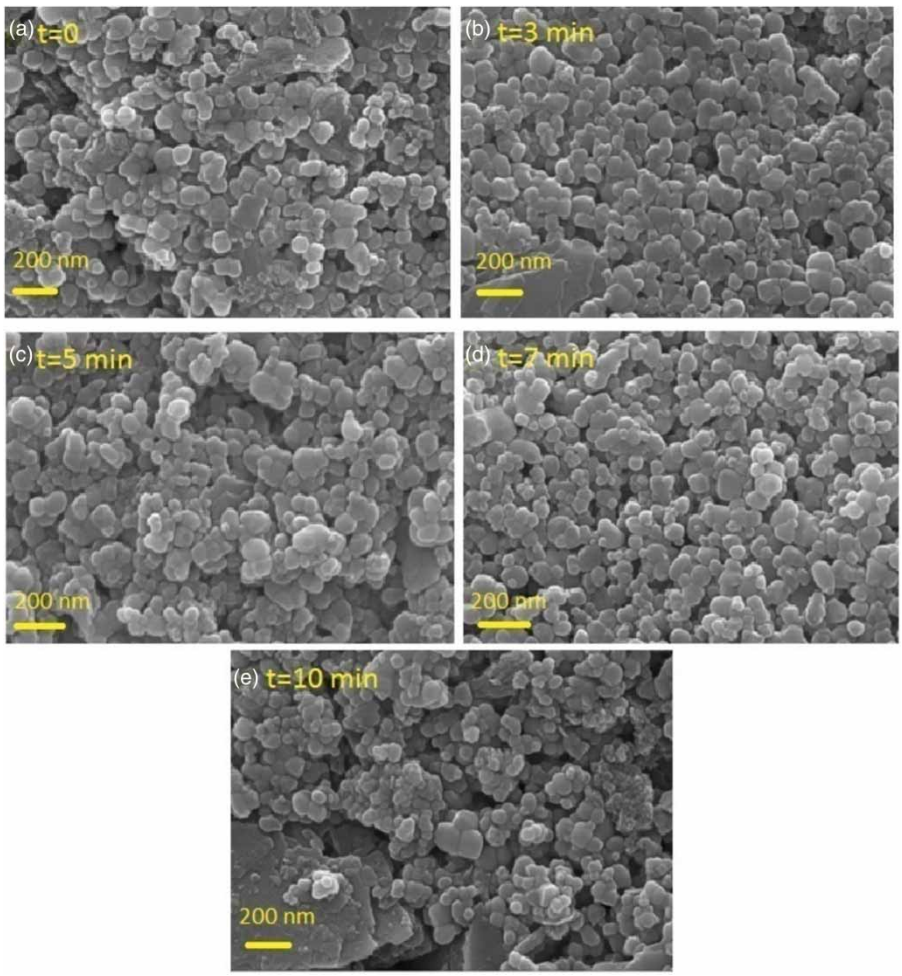

Figure 5 | SEM images at different irradiation times: (a) $t = 0$, (b) $t = 3$, (c) $t = 5$, (d) $t = 7$ and (e) $t = 10$ min.

Table 2 | EDX results of the nanocomposite samples at different irradiation times

Time (min)	O	Al	Si	K	Ca	Ti
0 (laser off)	50.68	2.38	15.58	0.32	0.72	30.31
3	47.67	4.80	28.8	0.86	1.37	16.50
5	52.04	6.15	33.00	0.98	2.62	5.21
7	48.78	5.97	39.21	1.32	1.41	3.32
10	49.56	1.15	4.27	0.04	0.51	44.48

(532 nm). The weight and atomic percentage of Si, Al, K, Ca and Ti from EDX analysis are shown in Table 2. It can be observed that the TiO_2 is homogeneously distributed all over the Zeolite matrix. The particle size decreases with increasing laser irradiation time as inferred from the SEM images. This observation confirms the results derived from the DLS analysis (Table 1). As seen in Figure 5(e), the nanocomposites were agglomerated and formed bigger particles.

EDX analysis proves that by increasing irradiation time, the amount of Si, Al, Ca and K in the Zeolite increased while the weight and atomic percentages of Ti in the nanocomposite decreased throughout the synthesis process. In comparison with the other analysis, these results for $t =$ 10 min are the reverse. Figure 6 shows EDX images for t = 0, 7 and 10 min irradiation time which indicate that Titanium has entered into the Zeolite structure in the nanocomposite.

According to the results, the optimum size was achieved by 7 min laser irradiation. This parameter for irradiation time was chosen for the photocatalytic experiments.

Photocatalytic activity of TiO_2–Zeolite nanocomposite

The removal of 2,4-D was evaluated under UV irradiation (12 W) and Xe lamp irradiation (200 W). Electron (e^-)–hole (h^+) pairs are generated on the surface of TiO_2 under UV irradiation which further react with O_2 and H_2O to produce reactive oxygen species (superoxide radicals ($O^{\bullet 2-}$) and hydroxide radicals ($OH^{\bullet -}$), respectively) in various chain reactions. These active species will degrade the structure of organic molecules. In the degradation of 2,4-D ($C_8H_6Cl_2O_3$), the $OH^{\bullet -}$ species produced from the reaction of light activated and adsorbed water at the surface of TiO_2 particles, which plays a significant role in the elimination of 2,4-D.

Figure 7(a) displays the effect of UV irradiation (12 W) on 2,4-D removal by pure anatase TiO_2, pure Zeolite, and TiO_2–Zeolite nanocomposite. It can be seen that 2,4-D removal is 9.07% for TiO_2, 18.68% for Zeolite, and 71.03%

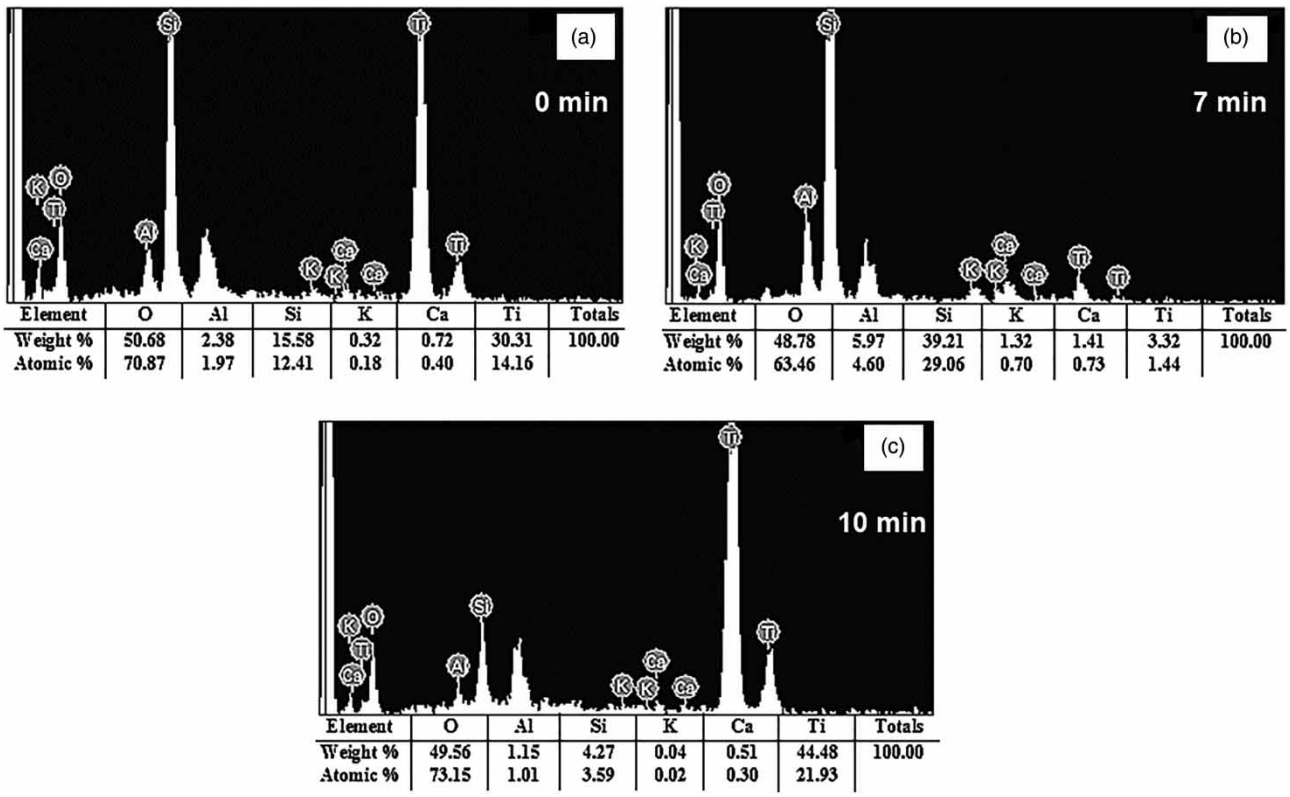

Figure 6 | EDX images at different irradiation times (a) $t = 0$, (b) $t = 7$ and (c) $t = 10$ min.

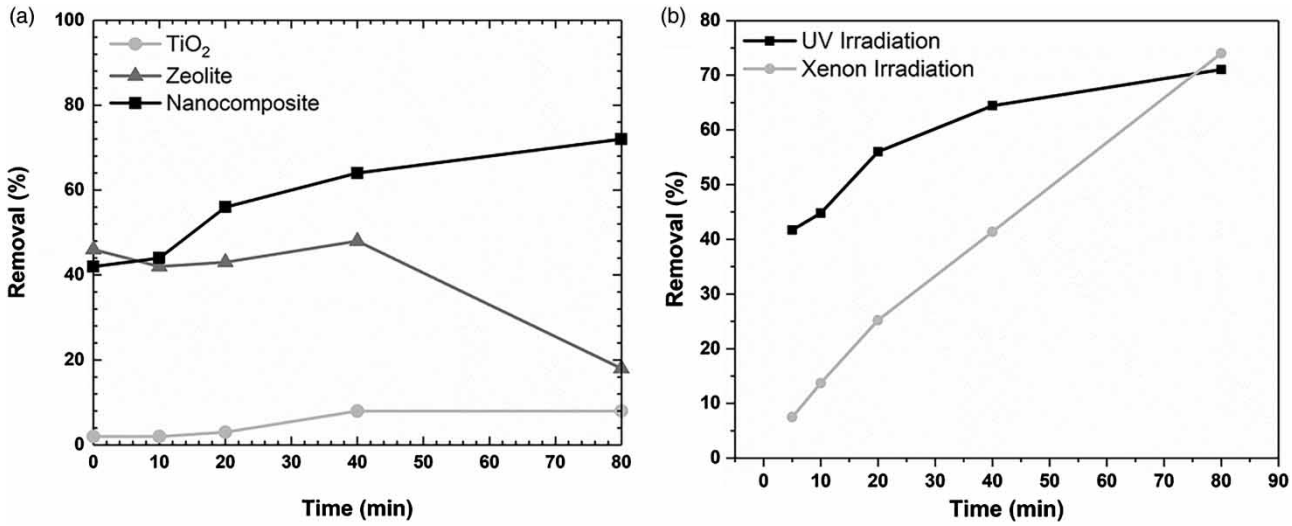

Figure 7 | (a) Removal of the 2,4-D by nanocomposite, pure Zeolite, and pure TiO_2 under UV irradiation; (b) comparison of 2,4-D removal by the nanocomposite under UV and Xe irradiation at different times.

for TiO_2–Zeolite nanocomposite (7 min laser irradiation (532 nm)) after 80 min. The effect of TiO_2–Zeolite nanocomposite in eliminating 2,4-D under UV irradiation (12 W) is much stronger compared with pure TiO_2 and pure Zeolite. All photocatalytic experiments were repeated four times, and the error bar for the experiment was found to be 0.06%.

For the removal process, the following mechanism for emerging pollutant species is suggested. First, 2,4-D herbicide decomposes into an ether form ($C_6H_3Cl_2OOH$) which later forms phenolic structures [C_6H_3Cl (OH)], [C_6H_3 $(OH)_3$]. Eventually, the transient species transform to the acetic acid and formic acid forms (CH_3-COOH, H-COOH), which finally release CO_2 according to the general equation (Herrmann & Guillard 2000):

$$C_8H_6Cl_2O_3 \longrightarrow C_6H_3Cl_2OOH \longrightarrow [C_6H_3Cl\ (OH)],\ [C_6H_3(OH)_3] \longrightarrow CH_3\text{-}COOH \longrightarrow H\text{-}COOH \longrightarrow CO_2 \quad (2)$$

Figure 7(a) displays the 2,4-D removal of the nanocomposite, pure Zeolite, and pure TiO_2. When the solutions were prepared, first they were stirred in the dark with a magnetic stirrer for 30 min. Since Zeolite is porous, it absorbed the 2,4-D. Therefore, when it was exposed to UV irradiation (12 W), absorption did not start from zero. For TiO_2 there was no absorption at $t = 0$.

The 2,4-D removal with zeolite without TiO_2 is accomplished only via sorption phenomena and not via the photocatalytic method. In the sorption method before UV irradiation, the sorption capacity of 2,4-D by anatase TiO_2 was low and considerably improved by zeolite adsorption (Setthaya *et al.* 2017). However, after 40 min, the porosity of zeolite is saturated and absorption does not occur, so the removal rate is reduced. The main reason for this reduction after 40 min can be attributed to the desorption of 2,4-D on Zeolite in solution. The results authenticated that the synthesis of TiO_2–Zeolite nanocomposite has remarkable advantages such as the high efficiency of the removal of 2,4-D compared with pure Zeolite and pure TiO_2.

Figure 7(b) shows that the Xe lamp irradiation (200 W) increased the removal rate of 2,4-D up to 74.02% compared with the 71.03% removal of UV irradiation (12 W) during 80 min.

It is commonly accepted that TiO_2 is an n-type semiconductor with a 3.2 eV band gap, and is considered to have one of the best photocatalytic activities in the near ultraviolet region.

However, it has good photodegradation properties under visible light while loaded into the Zeolite. The incorporation of TiO_2 into the Zeolite framework has a significant influence on the light absorption. The Kubelka–Munk relation can evaluate the value of the band gap energies of the prepared composites. The equation is as follows:

$$(\alpha h\nu)^n = A(h\nu - Eg) \quad (3)$$

where α is the absorption coefficient, $h\nu$ is light frequency, Eg is band gap energy, A is a constant and n is 2 or 1/2 for the allowed direct or indirect transitions, respectively. A plot obtained via $(\alpha h\nu)^2$ vs $h\nu$ and $(\alpha h\nu)^{1/2}$ vs $h\nu$ based on the direct and indirect transition is presented in Figure 8. The band gap energy value of the samples was estimated to be

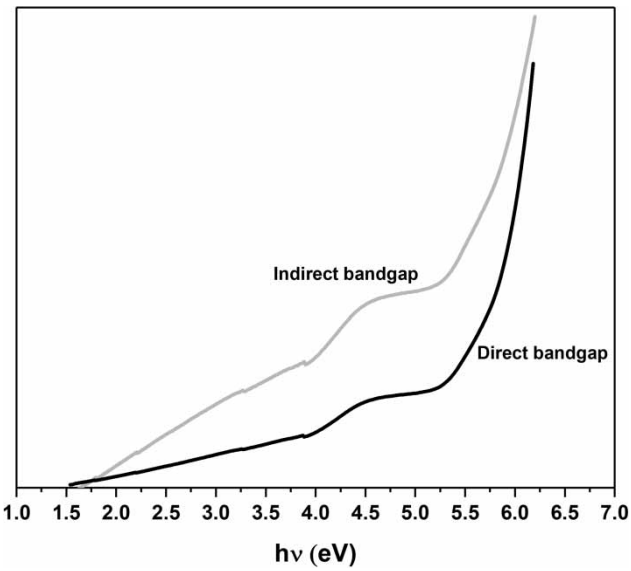

Figure 8 | Direct (*green*) and indirect (*red*) optical band gap of TiO_2–Zeolite nanocomposite. Please refer to the online version of this paper to see this figure in colour: http://dx.doi.org/10.2166/wst.2019.333.

1.5 eV and 1.7 eV for the direct and indirect transition, respectively. However, the estimated band gap value of the TiO_2–Zeolite nanocomposite is smaller than the value for TiO_2 (3.2 eV).

It can be seen that the absorption intensity of the TiO_2–Zeolite is higher in the visible region. The result of the band gap suggests that the removal of 2,4-D can be evaluated under Xe lamp irradiation (200 W) by the TiO_2–Zeolite nanocomposite.

Reusability of TiO_2–Zeolite nanocomposite

The reusability of the TiO_2–Zeolite nanocomposite was tested for four repetitive cycles. As observed, photocatalytic activity did not alter removal capacity after two cycles. After four runs of the experiments, the reduction in the catalytic performance was about 20%. This decrease in photocatalytic activity after four cycles can be attributed to the loss of photocatalyst during the washing process (Tobajas *et al.* 2017). In addition, the decline of the active sites of the TiO_2–Zeolite nanocomposite could be the other proof of this reduction (Jaafarzadeh *et al.* 2017). These data confirmed the durability of the photocatalyst in the reaction status employed in this study.

Comparison of the TiO_2–Zeolite nanocomposite with other photocatalysts

Lee *et al.* (2016) investigated the photocatalytic removal of 2,4-D herbicide using CuO–TiO_2 nanoparticles, and they achieved a 38% removal rate and 3.3 eV band gap energy, which is in the UV range. Abdennouri *et al.* (2015) fabricated Pt/TiO_2 nanoparticles with a 2.5 eV band gap which had a low removal efficiency for 2,4-D. Chenchana *et al.* (2018) obtained high removal of 2,4-D by Au–TiO_2(B)/anatase nanobelts with the band gap higher than 3.0 eV under UV irradiation. Oladipo (2018) achieved a 70% reduction of 2,4-D in the presence of 75 mg MIL-53(Fe) with a band gap of about 2.75 eV. In this study, the critical point is the band gap narrowing and shifting to visible region absorption and its photocatalytic activity. The removal efficiency of 2,4-D by TiO_2–Zeolite nanocomposite was remarkable compared with the reported literature.

CONCLUSION

In this study, a composite of TiO_2 particles with anatase phase and natural Zeolite was synthesized via a simple and cost-effective method known as a sol–gel method. The effect of laser irradiation time on the structure and size of the TiO_2–Zeolite nanocomposite was investigated, which showed a reduction in its size. From 3 min to 7 min laser irradiation time the particle size decreased except for 10 min, when the size of the nanocomposite increased unexpectedly. This phenomenon is ascribed to the nanocomposite's agglomeration. The smallest particle size was observed for 7 min laser irradiation, which was about 157 nm. The TiO_2–Zeolite nanocomposite band gap was calculated as 1.5 eV, which was lower than for pure TiO_2. The band gap reduction could be a substantial implication that the TiO_2–Zeolite nanocomposite had more absorption in the visible range. The most important application for such a nanocomposite is photocatalytic degradation that can facilitate water pollutant removal. The result from photodegradation of 2,4-D by the TiO_2–Zeolite nanocomposite was 71.03% and 74.02% under UV irradiation (12 W) and Xe lamp irradiation (200 W) during 80 min, respectively. The TiO_2–Zeolite nanocomposite also showed a remarkable stability after four cycling repetitions of the experiment. This novel, secure and cost-effective method to synthesize the nanocomposite is suggested in this study.

REFERENCES

Abdennouri, M., Elhalil, A., Farnane, M., Tounsadi, H., Mahjoubi, F. Z., Elmoubarki, R., Sadiq, M., Khamar, L., Galadi, A., Baâlala, M., Bensitel, M., El hafiane, Y., Smith, A. & Barka, N.

2015 Photocatalytic degradation of 2,4-D and 2,4-DP herbicides on Pt/TiO_2 nanoparticles. *Journal of Saudi Chemical Society* **19**, 485–493.

Agricultural Ministry 2012 *Agricultural Statistic Report 1391*. Agricultural Ministry, Tehran, Iran.

Anpo, M., Shima, T., Kodama, S. & Kubokawa, Y. 1987 Photocatalytic hydrogenation of propyne with water on small-particle titania: size quantization effects and reaction intermediates. *Journal of Physical Chemistry* **91** (16), 4305–4310.

Chenchana, A., Nemamcha, A., Moumeni, H., Doña Rodríguez, J. M., Araña, J., Navío, J. A., González Díaz, O. & Pulido Melián, E. 2018 Photodegradation of 2,4-dichlorophenoxyacetic acid over TiO_2(B)/anatase nanobelts and Au-TiO_2(B)/ anatase nanobelts. *Applied Surface Science* **467–468**, 1076–1087.

Cheng, X. W., Liu, H. L., Chen, Q. H., Li, J. J. & Wang, P. 2014 Preparation of graphene film decorated TiO_2 nano-tube array photoelectrode and its enhanced visible light photocatalytic mechanism. *Carbon* **66**, 450–458.

Chong, M. N., Vimonses, V., Lei, S., Jin, B., Chow, C. & Saint, C. 2009 Synthesis and characterisation of novel titania impregnated kaolinite nano-photocatalyst. *Microporous and Mesoporous Materials* **117**, 233–242.

Deveau, P.-A., Arsac, F., Thivel, P.-X., Ferronato, C., Delpech, F., Chovelon, J.-M., Kaluzny, P. & Monnet, C. 2007 Different methods in TiO_2 photodegradation mechanism studies: gaseous and TiO_2-adsorbed phases. *Journal of Hazardous Materials* **144**, 692–697.

Ding, L., Lu, X., Deng, H. & Zhang, X. 2012 Adsorptive removal of 2,4-dichlorophenoxyacetic acid (2,4-D) from aqueous solutions using MIEX resin. *Industrial & Engineering Chemistry Research* **51** (34), 11226–11235.

Haque, F. Z., Nandanwar, R. & Singh, P. 2017 Evaluating photodegradation properties of anatase and rutile TiO_2 nanoparticles for organic compounds. *Optik: International Journal for Light and Electron Optics* **128**, 191–200.

Hassan Alwash, A., Zuhairi Abdullah, A. & Ismail, N. 2013 Elucidation of reaction behaviors in sonocatalytic decolorization of amaranth dye in water using zeolite Y co-incorporated with Fe and TiO_2. *Advances in Chemical Engineering and Science* **3**, 113–122.

Herrmann, J.-M. & Guillard, C. 2000 Photocatalytic degradation of pesticides in agricultural used waters. *Comptes Rendus de l'Académie des Sciences – Series IIC – Chemistry* **3** (6), 417–422.

Jaafarzadeh, N., Ghanbari, F. & Ahmadi, M. 2017 Catalytic degradation of 2,4-dichlorophenoxyacetic acid (2,4-D) by nano-Fe_2O_3 activated peroxymonosulfate: influential factors and mechanism determination. *Chemosphere* **169**, 568–576.

Jaafarzadeh, N., Ghanbari, F. & Zahedi, A. 2018 Coupling electrooxidation and oxone for degradation of 2,4-dichlorophenoxyacetic acid (2,4-D) from aqueous solutions. *Journal of Water Process Engineering* **22**, 203–209.

Kamat, P. V., Flumiani, M. & Hartland, G. V. 1998 Picosecond dynamics of silver nanoclusters: photoejection of electrons and fragmentation. *Journal of Physical Chemistry B* **102**, 3123–3128.

la Farré, M., Pérez, S., Kantiani, L. & Barceló, D. 2008 Fate and toxicity of emerging pollutants, their metabolites and transformation products in the aquatic environment. *TrAC Trends in Analytical Chemistry* **27** (11), 991–1007.

Lee, S. C., Hasan, N., Lintang, H. O., Shamsuddin, M. & Yuliati, L. 2016 Photocatalytic removal of 2,4-dichlorophenoxyacetic acid herbicide on copper oxide/titanium dioxide prepared by co-precipitation method. *IOP Conference Series: Materials Science and Engineering* **107**, 012012.

Lemus, M. A., López, T., Recillas, S., Frías, D. M., Montes, M., Delgado, J. J., Centeno, M. A. & Odriozola, J. A. 2008 Photocatalytic degradation of 2,4-dichlorophenoxyacetic acid using nanocrystalline cryptomelane composite catalysts. *Journal of Molecular Catalysis A: Chemical* **281**, 107–112.

Liu, X., Iu, K. & Thomas, J. K. 1993 Preparation, characterization and photoreactivity of titanium (IV) oxide encapsulated in zeolites. *Journal of the Chemical Society, Faraday Transactions* **89** (11), 1861–1865.

Liu, S., Lim, M. & Amal, R. 2014 TiO_2-coated natural zeolite: rapid humic acid adsorption and effective photocatalytic regeneration. *Chemical Engineering Science* **105**, 46–52.

Nejati, K., Davary, S. & Saati, M. 2013 Study of 2,4-dichlorophenoxyacetic acid (2,4-D) removal by Cu-Fe-layered double hydroxide from aqueous solution. *Applied Surface Science* **280**, 67–73.

Oladipo, A. A. 2018 MIL-53 (Fe)-based photo-sensitive composite for degradation of organochlorinated herbicide and enhanced reduction of Cr(VI). *Process Safety and Environmental Protection* **116**, 413–423.

Sendova, M., Sendova-Vassileva, M., Pivin, J. C., Hofmeister, H., Coffey, K. & Warren, A. 2006 Experimental study of interaction of laser radiation with silver nanoparticles in SiO_2 matrix. *Journal of Nanoscience and Nanotechnology* **6**, 748–755.

Setthaya, N., Chindaprasirt, P., Yin, S. & Pimraksa, K. 2017 TiO_2-zeolite photocatalysts made of metakaolin and rice husk ash for removal of methylene blue dye. *Powder Technology* **313**, 417–426.

Taheri Najafabadi, A. & Taghipour, F. 2014 Physicochemical impact of zeolites as the support for photocatalytic hydrogen production using solar-activated TiO_2-based nanoparticles. *Energy Conversion and Management* **82**, 106–113.

Tobajas, M., Belver, C. & Rodriguez, J. J. 2017 Degradation of emerging pollutants in water under solar irradiation using novel TiO_2-ZnO/clay nanoarchitectures. *Chemical Engineering Journal* **309**, 596–606.

Trujillo, M. E., Hirales, D., Rincón, M. E., Hinojosa, J. F., Leyva, G. L. & Castillón, F. F. 2013 TiO_2/clinoptilolite composites for photocatalytic degradation of anionic and cationic contaminants. *Journal of Materials Science* **48**, 6778–6785.

Yener, H. B., Yılmaz, M., Deliismail, Ö., Özkan, S. F. & Helvacı, Ş. Ş. 2017 Clinoptilolite supported rutile TiO_2 composites: synthesis characterization, and photocatalytic activity on the degradation of terephthalic acid. *Separation and Purification Technology* **173**, 17–26.

First received 18 March 2019; accepted in revised form 15 September 2019. Available online 30 September 2019